

The First Metal Complexes of the Proton Sponge 1,8-Bis(*N,N,N',N'*-tetramethylguanidino)naphthalene: Syntheses and Properties

Ute Wild,^[a] Olaf Hübner,^[a] Astrid Maronna,^[a] Markus Enders,^[a] Elisabeth Kaifer,^[a] Hubert Wadepohl,^[a] and Hans-Jörg Himmel^{*[a]}

Keywords: Proton sponge / Coordination compounds / Palladium / Platinum / Guanidine / Chelates

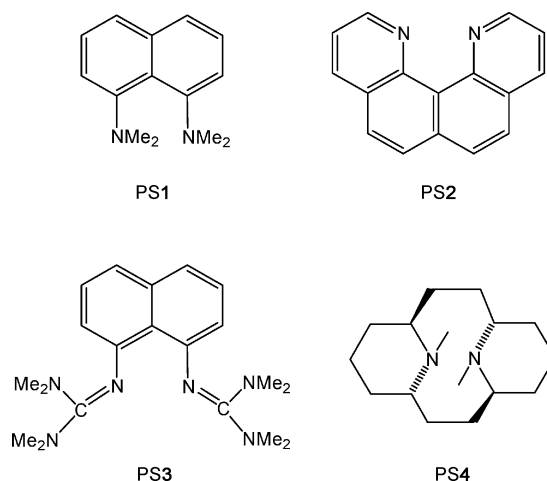
In this work we report on the syntheses and properties of the first transition metal complexes of the proton sponge 1,8-bis(*N,N,N',N'*-tetramethylguanidino)naphthalene (btmgn). Of the three complexes [(btmgn)PdCl₂], [(btmgn)PtCl₂] and [(btmgn)PtCl₂(C₂H₄)], the first two feature a chelating btmgn ligand that is bound to the metal atom through two nitrogen atoms. Only one metal–N bond is established in [(btmgn)PtCl₂(C₂H₄)]. The molecular structures of [(btmgn)PdCl₂] and [(btmgn)PtCl₂] show some interesting details. X-ray crystallographic studies reveal that the naphthyl aromatic systems in both complexes are not planar, the metal atoms reside above the “best-plane” of the naphthyl systems and the compounds adopt a chiral conformation in the crystalline phase.

Several dynamic processes of the two guanidinyll groups in solution were identified by line-shape analysis of the temperature-dependent NMR spectra. The complex [(btmgn)PtCl₂(C₂H₄)] eliminates ethylene at elevated temperature to give [(btmgn)PtCl₂]. Quantum chemical (DFT) calculations indicate that the Δ*G*⁰ value for this reaction is close to zero. Indeed the compound [(btmgbp)PtCl₂] {btmgbp = 2,2'-bis(*N,N,N',N'*-tetramethylguanidino)biphenyl} in which the naphthyl group is replaced by a biphenyl group is not amenable to ethylene elimination. First experiments point to interesting catalytic properties of the new complexes. (© Wiley-VCH Verlag GmbH & Co. KGaA, 69451 Weinheim, Germany, 2008)

Introduction

The first example of a proton sponge, 1,8-bis(dimethylamino)naphthalene (PS1) (see Scheme 1), was reported in 1968 by Alder et al.^[1] and features two dimethylamino groups in close proximity. While PS1 has a high affinity towards H⁺, it is indifferent to other electrophiles, which is in contrast to usual nitrogen bases. This implies that PS1 is not ready to act as ligand in coordination complexes. Indeed, up to date only one complex^[2] of the archetypal proton sponge PS1 is known.^[3] Other examples for proton sponges include quino[7,8-*h*]quinoline (PS2)^[4] and 1,8-bis(*N,N,N',N'*-tetramethylguanidino)naphthalene (PS3).^[5] On the basis of quantum chemical calculations, PS4 was suggested to be a superior chiral proton sponge.^[6] However, its synthesis has not yet been achieved. Recently, the first transition metal complexes of the proton sponge PS2 were reported.^[7] Herein we report the syntheses, characterization and reactivity of the first metal complexes of the proton sponge PS3 that exhibit unusual structures and interesting reactivity. Complex formation in the case of PS3 is easier than for PS1 because the lone pairs at the imine-nitrogen

atoms of PS3 are sterically less shielded than the nitrogen lone pairs in PS1. Many transition metal complexes featuring ligands with tetramethylguanidino groups were synthesized in the recent years. Because of the strong basicity of guanidines, interesting properties are expected for these complexes. To name two examples, Henkel et al. synthesized several complexes (especially of Fe and Cu) of bis-guanidines, using e.g. 1,3-bis(*N,N,N',N'*-tetramethylguanidino)propane [(Me₂N)₂CN(CH₂)₃CN(NMe₂)₂]^[8] and also published valuable work on the synthetic routes to such ligands.^[9] Very recently, the first 1:1 Cu/O₂ complex featuring



Scheme 1.

[a] Anorganisch-Chemisches Institut, Ruprecht-Karls-Universität Heidelberg, Im Neuenheimer Feld 270, 69120 Heidelberg, Germany Fax: +49-6221-54-5707 E-mail: hans-jorg.himmel@aci.uni-heidelberg.de Supporting information for this article is available on the WWW under <http://www.eurjic.org> or from the author.

end-on coordinated O₂ was reported.^[10] In this complex, Cu is coordinated by the tripodal, superbasic and sterically encumbered tris(tetramethylguanidino)tren (tmg3tren) ligand.

Results and Discussion

Reaction of [(1,5-cod)PdCl₂] (1,5-cod = 1,5-cyclooctadiene) and PS3 in CH₂Cl₂ yielded the new Pd complex [(PS3)PdCl₂] (**1**). Red crystals suitable for X-ray diffraction

were obtained from CH₂Cl₂/Et₂O solutions. The molecular structure of **1** is illustrated in Figure 1. Selected structural parameters can be found in Table 1. The most remarkable features of the structure are the non-planarity of the naphthalene aromatic system and the location of the Pd atom 133.8(7) pm above the “best plane” of the aromatic system.^[11] Furthermore, **1** is chiral (see Figure 1) and contains two pairs of enantiomers in the unit cell.

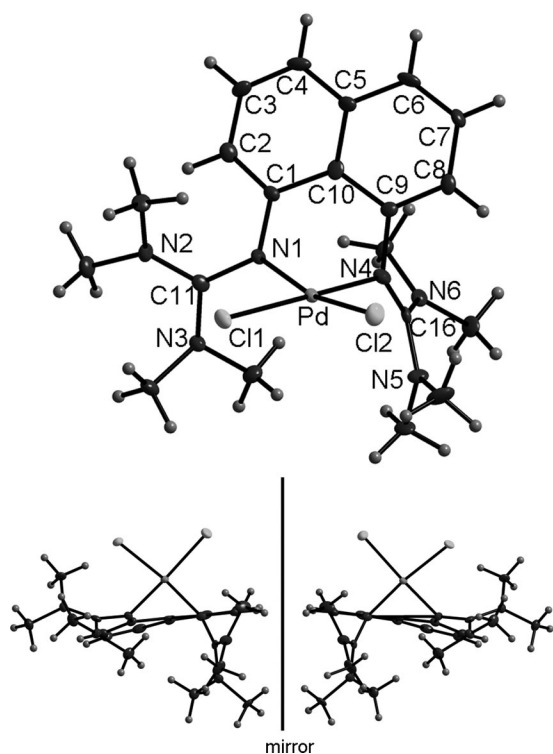


Figure 1. Molecular structure of complex **1** (in front view and the two enantiomers in side view). Ellipsoids are drawn at the 50% probability level.

Table 1. Selected bond lengths [pm] and angles [°] for **1**.

Pd–Cl1	232.62(13)	Pd–Cl2	231.09(16)
Pd–N1	205.3(5)	Pd–N4	201.0(5)
N1–C1	140.6(7)	N4–C9	143.2(7)
N1–C11	135.2(7)	N4–C16	132.4(7)
C11–N2	135.8(8)	C16–N6	135.1(7)
C11–N3	134.1(7)	C16–N5	135.4(8)
C1–C10	146.0(8)	C9–C10	143.6(8)
C1–C2	138.6(8)	C8–C9	136.8(8)
C4–C5	141.1(9)	C5–C6	142.4(9)
C3–C4	136.0(9)	C6–C7	135.8(9)
C2–C3	139.5(8)	C7–C8	141.5(8)
C5–C10	142.4(8)		
C11–Pd–Cl2	89.53(6)	N1–Pd–N4	81.92(19)
C11–Pd–N1	92.84(14)	Cl2–Pd–N4	96.29(14)
C1–N1–Pd	116.5(4)	C9–N4–Pd	109.0(3)
C1–N1–C11	123.3(5)	C9–N4–C16	121.1(5)
C1–N1–C11–N2	–38.7	C1–N1–C11–N3	141.7

Variable low-temperature ¹H NMR studies of **1** were carried out to analyze the flexibility of the guanidinyll groups in solution (Figure 2). The ¹H NMR spectra at room temperature show a symmetric naphthalene unit (three resonances for *ortho*, *meta* and *para* H atoms) and one single resonance for the eight N–CH₃ groups. Upon cooling, the N–CH₃ signal splits into four signals and by further lowering of the temperature, the Pd complex **1** gives eight distinct signals for the methyl groups, and the *ortho* and *para* H atoms of the naphthalene moiety are split into two pairs of signals. This pattern is in accordance with the structure in the solid state, where the symmetry of the naphthalene unit

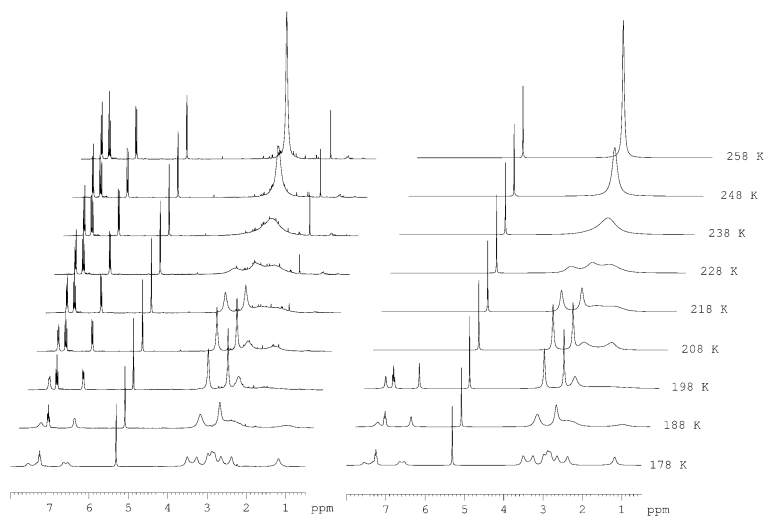
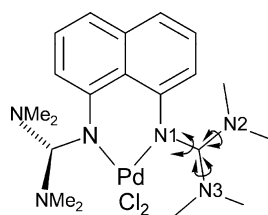


Figure 2. Experimental variable-temperature ¹H NMR spectra of **1** (left) and corresponding simulated spectra (right). The aromatic resonances were simulated only for the fast low-temperature process (178 K–198 K). The signal at $\delta = 5.3$ ppm arises from traces of CH₂Cl₂. For the corresponding rate constants see Table 2.

is lowered by the significantly different orientation of the two guanidine units. In order to get further insight into the dynamic processes, we simulated the variable-temperature ^1H NMR spectra with the aid of a line-shape analysis module^[12] and extracted rate constants by fitting the simulated spectra with the experimental spectra. As a result, three well-separated rate constants of four different fluxional processes have been determined. The fastest process which leads to a symmetric naphthalene unit and four N–CH₃ resonances can be described by reorientation of the two guanidine units without complete rotation around the N1–C bonds (see Scheme 2). The fitting of the rate constant for this process results in a value of 78 Hz at a temperature of 178 K. By further analysis of the line shape behavior a Gibbs free activation energy ΔG^\ddagger of 36 kJ mol⁻¹ has been determined. This process results in racemization of the enantiomeric complexes observed in the crystal. A complete rotation of the guanidine units can be ruled out, as this would lead to a spectrum with only two different N–CH₃ resonances. Rotation around the N2–C bond and the N3–C bond occurs at two different reaction rates. The slower rotation is accompanied by a complete rotation of the guanidine units (rotation around the N1–C bond, Scheme 2). Table 2 summarizes the results of the line-shape analysis.



Scheme 2.

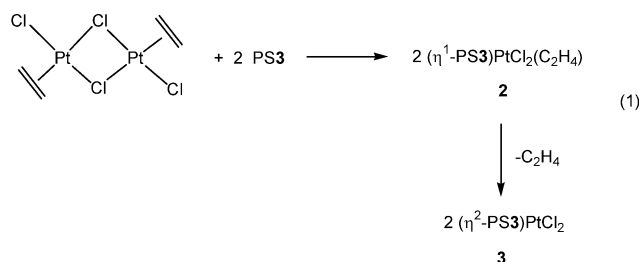
Table 2. Estimated rate constants and Gibbs free activation energy barriers ΔG^\ddagger for the different processes observed in the temperature-dependent NMR spectra.

T [K]	Rate constants [s ⁻¹]		
	Process 1 ^[a]	Process 2 ^[b]	Process 3 ^[c]
178	78		
188	300		
198	1150		
208		230	11
218		470	25
228		1000	100
238		4000	310
248		10000	920
258		20000	3500
ΔG^\ddagger [kJ mol ⁻¹]	36 (200 K)	42 (250 K)	46 (250 K)

[a] Reorientation of the guanidine units without complete rotation. [b] Rotation of NMe₂ unit. [c] Rotation of second NMe₂ unit. A simultaneous rotation around N1–C has been presumed with the same reaction rate for the simulation of this parameter.

First experiments aiming at the synthesis of Pt complexes of PS3 with the compound PtCl₂(dmsO)₂ as precursor gave no results. The only complex that could be isolated in small amounts was the salt [PS3H]⁺[PtCl₃(dmsO)]⁻. On the other

hand, reaction of Zeise's dimer [Pt₂(C₂H₄)₂Cl₄] with the hydrogen sponge PS3 in CH₂Cl₂ at room temperature gave the new complex **2** [see Equation (1)].



The NMR spectroscopic data of **2** indicates the presence of an ethylene unit. The isolation of an ethylene complex in the case of Pt but not Pd is in agreement with the larger stability of Pt^{II} alkene complexes compared to their Pd^{II} counterparts.^[13] Yellow crystals of the complex were obtained from toluene layered by petroleum ether (PE) 40/60 and Figure 3 illustrates the molecular structure as determined by X-ray diffraction (see Table 3 for selected structural parameters). Only one of the guanidinyll groups in **2** is bound to Pt. As in the [PtCl₃(C₂H₄)]⁻ anion of Zeise's salt,^[14] the ethylene moiety is oriented perpendicularly to the plane hosting the Pt atom, the two Cl atoms and the N atom attached to Pt. With a value of 135.7(9) pm, the C=C distance is, as anticipated, elongated with respect to that in free ethylene [133.7(2) pm].^[15] The two Pt–C distances are slightly different and have values of 213.8(7) and 211.9(6) pm, which are comparable with the Pt–C distances in Zeise's salt [212.8(3) and 213.5(3) pm]. The Pt–N distance in **2** is 206.9(4) pm. For comparison, in *cis*- and *trans*-[(hppH)₂PtCl₂] (hppH = 1,3,4,6,7,8-hexahydro-2*H*-pyrimido[1,2-*a*]pyrimidine) values of 202.2(3)/202.3(3) and 203.3(2) pm, respectively, were determined.^[16] The relatively large Pt–N distance in **2** can be explained by the strong *trans* effect of coordinated ethylene. Complex **2** is stable in toluene at room temperature. However, in refluxing CH₂Cl₂ it eliminates ethylene to give the new complex **3**. The NMR spectroscopic data of **3** shows the disappearance of the signals from the ethylene group. Orange crystals of **3** were grown by layering a CH₂Cl₂ solution with PE 40/60. The single-crystal X-ray diffraction analysis confirms that **3** is the homologue of **1**, namely the complex [(PS3)PtCl₂], in which both guanidinyll groups are bound to the Pt atom (see Figure 4 and Table 4). As a consequence of the η²-coordination mode, the naphthyl group again abandons its planar structure. Moreover, the Pt atom is located 133.1 pm above the “best plane” of the aromatic system.^[7] This unusual structure is in clear contrast to that of e.g. [(btmgb)-PtCl₂] (**4**) {btmgb = 1,2-bis(*N,N,N',N'*-tetramethylguanidino)benzene}, in which the Pt atom lies in the plane defined by the C₆ aromatic ring.^[17] Like its Pd analogue, **3** features two pairs of enantiomers in the unit cell. Some variable low-temperature ^1H NMR spectra recorded for this complex in solution are shown in Figure 5. As in the case of **1**, the spectrum at room temperature displays only one signal at $\delta = 2.83$ ppm for all eight methyl groups. However,

the splitting into four CH₃ signals occurs at lower temperature than in the case of **1** indicating more facile rotation around the C–N bonds of the guanidinyll groups. The spectrum recorded at 178 K still shows four signals, which means that the rate for interconversion of the two enantiomers is higher for **3** than for **1**. It is obvious that the bond order of the N=C double bonds in PS3 before coordination is considerably reduced after coordination relative not only to the free ligand but also to the situation in complex **1**. This is also manifested in the C1–N1–C11–N3 and C1–N1–C11–N2 torsion angles of 41.7° and –139.8°.

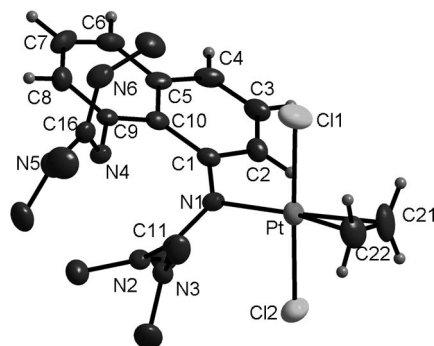


Figure 3. Molecular structure of complex **2**. Ellipsoids are drawn at the 50% probability level. The H atoms of the methyl groups were omitted for clarity.

Table 3. Selected bond lengths [pm] and angles [°] for **2**.

Pt–Cl1	229.63(15)	Pt–Cl2	230.35(15)
Pt–C21	213.8(7)	Pt–C22	211.9(6)
Pt–N1	206.9(4)	Pt...N4	458.5(3)
N1–C1	142.8(6)	N4–C9	139.9(6)
N1–C11	132.9(6)	N4–C16	129.0(6)
C11–N2	135.7(6)	C16–N5	137.3(7)
C11–N3	135.7(6)	C16–N6	139.6(7)
C1–C2	138.5(7)	C8–C9	138.2(7)
C2–C3	140.0(7)	C7–C8	139.2(8)
C3–C4	134.2(7)	C6–C7	135.2(8)
C4–C5	142.2(7)	C5–C6	142.2(8)
C1–C10	143.8(7)	C9–C10	144.4(7)
C5–C10	144.6(7)	C21–C22	135.7(9)
C21–H	97.4(19)/96(2)	C22–H	97.4(19)/97(2)
Cl1–Pt–Cl2	178.36(6)	C21–Pt–C22	37.2(3)
N1–Pt–Cl1	91.32(12)	N1–Pt–Cl2	89.56(12)
Cl1–Pt–C21	91.0(2)	Cl1–Pt–C22	87.9(2)
C1–N1–Pt	118.6(3)	Cl1–N1–Pt	120.6(3)
N1–C11–N2	122.6(4)	N1–C11–N3	120.2(4)
N2–C11–N3	117.1(5)	N4–C16–N5	120.7(5)
N4–C16–N6	125.9(5)	N5–C16–N6	113.3(4)

Quantum chemical calculations [18] suggest that the elimination of ethylene from **2** to give **3** is associated with a change in energy and Gibbs free energy (at 298 K, 1013 mbar) of 45.4 and –3.2 kJ mol^{–1}, respectively. Inspection of the isodensity surfaces (see Supporting Information) of the HOMO orbitals of **2** and **3** shows that the HOMO is concentrated at the PS3 ligand for **2**, but at the Pt and Cl atoms for **3**. In contrast, the LUMO is concentrated at Pt and Cl for **2** and at the PS3 ligand for **3**. The calculated ΔG^0 value close to zero for ethylene elimination from **2** to give **3** implies that even slight modifications in the back-

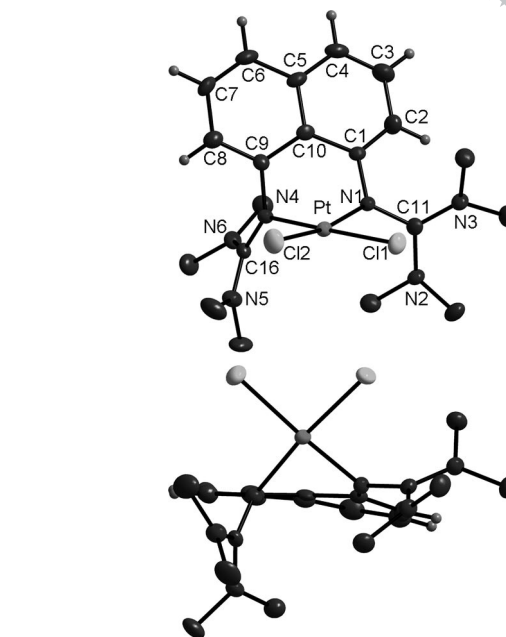


Figure 4. Molecular structure of complex **3** in front and side view. Ellipsoids are drawn at the 50% probability level. The H atoms of the methyl groups were omitted for clarity.

Table 4. Selected bond lengths [pm] and angles [°] for **3**.

Pt–Cl1	232.62(12)	Pt–Cl2	230.71(11)
Pt–N1	204.6(3)	Pt–N4	202.8(3)
N1–C1	141.6(5)	N4–C9	142.5(5)
N1–C11	135.7(5)	N4–C16	133.5(5)
C11–N2	134.3(5)	C16–N5	135.5(5)
C11–N3	134.5(5)	C16–N6	135.5(5)
C1–C2	138.4(5)	C8–C9	137.7(5)
C2–C3	140.3(6)	C7–C8	140.9(6)
C3–C4	136.4(6)	C6–C7	134.0(6)
C4–C5	140.7(6)	C5–C6	142.9(6)
C1–C10	145.6(5)	C9–C10	143.0(5)
C5–C10	142.6(5)		
Cl1–Pt–Cl2	88.50(4)	N1–Pt–N4	82.06(12)
Cl1–Pt–N1	92.45(9)	Cl2–Pt–N4	97.21(10)
C1–N1–Pt	117.6(2)	C9–N4–Pt	109.0(3)
N1–C11–N2	117.8(4)	N4–C16–N5	119.8(4)
N1–C11–N3	123.9(4)	N4–C16–N6	123.0(4)
N2–C11–N3	118.3(3)	N5–C16–N6	117.2(4)
C1–N1–C11–N2	–139.8	C1–N1–C11–N3	41.7

bone of the bisguanidino ligand system could turn ΔG^0 to positive values. To gain further insight, we prepared a related Pt ethylene complex, namely [(btmgbp)PtCl₂(C₂H₄)] (**5**) {btmgbp = 2,2'-bis(*N,N,N',N'*-tetramethylguanidino)-biphenyl}, in which the naphthyl group is replaced by biphenyl. Complex **5** can be obtained in a similar way as **2** from btmgbp and [Pt₂(C₂H₄)₂Cl₂], and Figure 6 displays its molecular structure (see Table 5 for selected structural parameters). Similar to the situation in **2**, the bisguanidino unit is bound only through one N atom to Pt. However, in this case even prolonged heating of a CH₂Cl₂ solution (and also of a CH₃CN solution) of **5** to reflux for 24 h did not cause formation of [(btmgbp)PtCl₂].

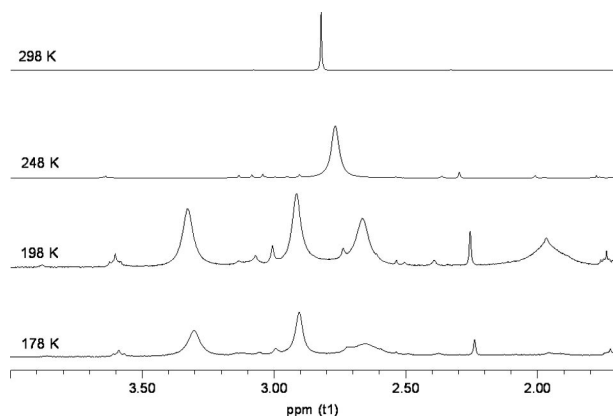


Figure 5. Experimental variable-temperature ^1H NMR spectra of **3**.

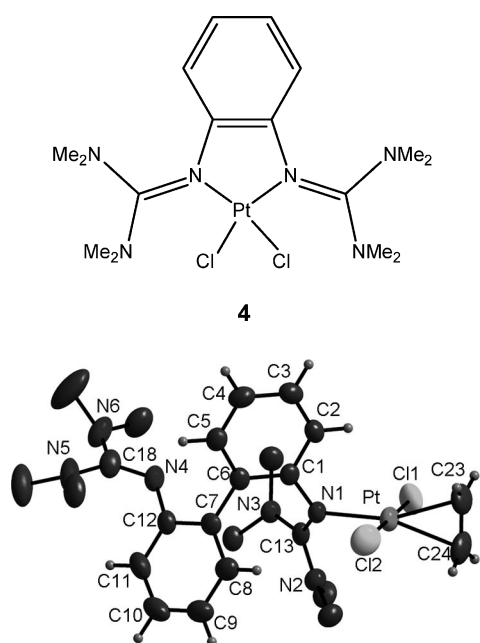


Figure 6. Molecular structure of complex **5**. Ellipsoids are drawn at the 50% probability level. The H atoms of the methyl groups were omitted for clarity.

Table 5. Selected bond lengths [pm] and angles [°] for **5**.

Pt–Cl1	229.23(13)	Pt–Cl2	2.3016(13)
Pt–C23	2.156(5)	Pt–C24	2.147(5)
Pt–N1	2.066(3)	Pt...N4	663.9(6)
N1–C1	1.430(4)	N4–C12	1.408(5)
N1–C13	1.333(4)	N4–C18	1.284(5)
C13–N2	1.346(5)	C18–N5	1.388(5)
C13–N3	1.343(4)	C18–N6	1.380(5)
C1–C6	1.404(5)	C7–C12	1.407(5)
C6–C7	1.484(5)		
Cl1–Pt–Cl2	178.41(4)	C23–Pt–C24	36.9(2)
N1–Pt–Cl1	87.95(8)	N1–Pt–Cl2	90.63(8)
Cl1–Pt–C23	89.8(2)	Cl1–Pt–C24	91.49(18)
C1–N1–Pt	116.3(2)	C13–N1–Pt	120.7(2)
N1–C13–N2	120.0(3)	N1–C13–N3	122.8(3)
N2–C13–N3	117.2(3)	N4–C18–N5	127.3(4)
N4–C18–N6	118.7(4)	N5–C18–N6	114.0(4)

As a consequence of the unusual molecular structures, interesting chemical properties are expected for the three complexes **1–3**. As first examples, we briefly inspected two different catalytic reactions: (i) Heck reaction between styrene and phenyl iodide to give *trans*-stilbene catalyzed by complex **1**. As detailed in the Experimental Section, complex **1** turned out to be a good catalyst for this reaction yielding nearly quantitative amounts of *trans*-stilbene. The number of turnovers was 45, and the turnover frequency [TOF, (mol product)/(mol catalyst \times time)] is roughly 9 h^{-1} . Thus, the process is quite fast, although catalysts with higher TOF are known.^[19] (ii) Hydrosilylation between Et_3SiH and $\text{Me}_3\text{SiC(H)CH}_2$ to give $\text{Me}_3\text{SiC(H)CH(SiEt}_3)$ at room temperature in the presence of the Pt complexes **2** or **3**. In this case we followed the product yield with GC/MS. The applied conditions were similar to that used previously in a study which compared the catalytic activity of several Pt^0 olefin complexes with that of the archetypical Karstedt catalyst.^[20] Our results (see Figure 7) show that complex **2** is a highly active catalyst for this reaction. The number of turnovers was ca. 500, and the turnover frequency can be estimated to be 302 h^{-1} from the plot shown in Figure 5 [for this estimate, the linear curve section (16–96 min) was used]. There was no sign of an induction period and the product yield reached >95% after less than 200 min. No colloid formation or precipitate was observed indicating a homogeneous process. Interestingly, complex **3** showed no or only very low catalytic activity, in contrast to **2**; even after 140 min no significant product formation was detectable. Only after addition of CH_2Cl_2 (increasing the solubility of **3**) the reaction started slowly with ca. 10% yield after 550 min.

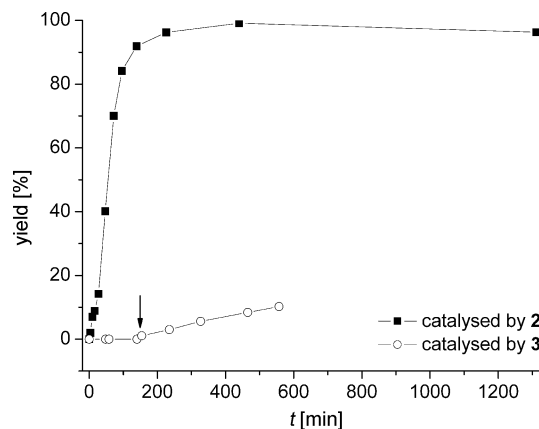


Figure 7. Product yield (according to GC/MS) in the hydrosilylation reaction between Et_3SiH and $\text{Me}_3\text{SiCH}_2\text{CH}_3$ to give $\text{Me}_3\text{SiC(H)CH}_2\text{(SiEt}_3)$ using complex **2** and **3** as catalyst. The arrow marks the point at which CH_2Cl_2 was added to increase the solubility of complex **2**.

Conclusions

In this work we report the syntheses of the first transition metal complexes of the proton sponge 1,8-bis(*N,N,N',N'*-tetramethylguanidino)naphthalene (btmgn). In the com-

plexes [(btmgn)PdCl₂] (**1**) and [(btmgn)PtCl₂] (**3**), the btmgn ligand acts as a chelating ligand, that is bound to the metal atom through two nitrogen atoms. The most remarkable structural features of both complexes [(btmgn)PdCl₂] and [(btmgn)PtCl₂] are the non-planarity of the naphthyl aromatic system, the location of the metal atom above the “best plane” of the aromatic systems, and the chirality of the molecules in the crystalline phase. A line-shape analysis of dynamic NMR spectra showed that ca. 80 interconversions per second between the two enantiomers of [(btmgn)-PdCl₂] occur already at 178 K ($\Delta G^\ddagger \approx 36 \text{ kJ mol}^{-1}$), making an isolation of one enantiomer virtually impossible. In the case of [(btmgn)PtCl₂], the interconversion is even faster. The NMR studies also provide information about the rates and Gibbs free energies for rotations around the guanidiny C–N bonds.

In contrast to the situation in [(btmgn)PdCl₂] and [(btmgn)PtCl₂], only one N–Pt bond is established in the complex [(btmgn)PtCl₂(C₂H₄)] (**2**), which eliminates ethylene at elevated temperatures to give [(btmgn)PtCl₂]. Quantum chemical (B3LYP) calculations predict a ΔG^0 value (at 298 K, 1 bar) of not more than -3.2 kJ mol^{-1} for this process. To obtain further information, the compound [(btmgbp)PtCl₂(C₂H₄)] was synthesized. Elimination of C₂H₄ should be less favorable in this case (formation of a seven-membered ring), and indeed this reaction is not observed.

Finally, first catalytic tests were carried out on [(btmgn)-PdCl₂], [(btmgn)PtCl₂], and [(btmgn)PtCl₂(C₂H₄)]. Although much more research is necessary to fully explore the catalytic potential of these complexes, these preliminary tests show interesting results. Heck reactions with [(btmgn)-PdCl₂] proceed smoothly, although catalysts with larger turn-over frequencies are known. The most remarkable result is that [(btmgn)PtCl₂(C₂H₄)] seems to be a good catalyst for hydrosilylation reactions (TOF of ca. 300 h⁻¹), while [(btmgn)PtCl₂] does not seem to catalyze hydrosilylation.

Experimental Section

All reactions were carried out under a dry argon atmosphere using standard Schlenk techniques. All solvents were dried using the standard methods followed by distillation. [(1,5-cod)PdCl₂] was either prepared from dichloridobis(benzonitrile)palladium(II) (99% purity, ABCR) or purchased from ABCR (99% purity). For the synthesis of [(1,5-cod)PdCl₂], 1,5-cod (0.9 mL, 7.3 mmol) was added to dichloridobis(benzonitrile)palladium(II) (50 mg, 0.13 mmol). The solution was carefully heated with a heat gun for some time until reflux. Afterwards, it was stirred for 1 h at room temperature. PS3 and the dinuclear complex di- μ -chlorido-dichloridobis(ethylene)diplatinum(II) [PtCl(C₂H₄)(μ -Cl)]₂ used in the syntheses of the Pt complexes were purchased from Fluka (purity) and ABCR (97% purity), respectively. IR spectra were recorded with a BIORAD Excalibur FTS 3000 spectrometer. NMR spectra were measured with a Bruker Avance II 400 spectrometer. The variable-temperature NMR measurements were recorded with a Bruker DRX 300 spectrometer. A Perkin–Elmer Lambda 19 spectrometer was used to obtain UV/Vis spectroscopic data.

X-ray Crystallographic Studies: Suitable crystals were taken directly out of the mother liquor, immersed in perfluorinated polyether oil, and fixed on top of a glass capillary. Measurements were performed at low temperature with a Bruker AXS Smart 1000 diffractometer and with a Nonius-Kappa CCD diffractometer (Mo- K_α radiation, graphite monochromated, $\lambda = 0.71073 \text{ \AA}$). The data collected were processed using the standard Bruker and Nonius software.^[21] The structures were solved by the heavy atom method combined with structure expansion by direct methods applied to difference structure factors (complex **1**)^[22] or by conventional direct methods^[23] and refined by full-matrix least-squares methods based on F^2 against all reflections.^[19] All non-hydrogen atoms were given anisotropic displacement parameters. Hydrogen atoms were fixed at calculated positions and refined with a riding model. CCDC-686257 (compound **1**), -686258 (compound **2**), -686259 (compound **3**) and -693423 (compound **5**) contain the supplementary crystallographic data (excluding structure factors) for this paper. These data can be obtained free of charge from The Cambridge Crystallographic Data Centre via http://www.ccdc.cam.ac.uk/data_request/cif.

[(PS3)PdCl₂] (1**):** [(1,5-cod)PdCl₂] (30 mg, 0.11 mmol) was dissolved in CH₂Cl₂ (10 mL) and stirred under reflux. PS3 (56 mg, 0.16 mmol, 0.145 equiv.) in CH₂Cl₂ (10 mL) was added dropwise to this solution over a period of 30 min. The orange-colored clear solution was stirred for additional 2 h and afterwards filtered through a silica frit. The solvent was removed in vacuo and the orange residue was washed several times with diethyl ether and PE 40/60 yielding an orange powder. Red crystals (27 mg, 47%) of **1** were obtained by layering a CH₂Cl₂ solution of this powder with diethyl ether. C₂₀H₃₀Cl₂N₆Pd (531.80): calcd. C 45.17, H 5.69, N 15.80; found C 44.34, H 5.65, N 15.21. ¹H NMR (399.89 MHz, CD₂Cl₂, 296.2 K): $\delta = 7.497$ (d, ¹J_{H-H} = 8.1 Hz, 2 H), 7.30 (t, ¹J_{H-H} = 7.8 Hz, 2 H), 6.61 (s, ¹J_{H-H} = 7.5 Hz, 2 H), 2.82 (s, 24 H, CH₃) ppm. ¹³C NMR (100.56 MHz, CD₂Cl₂, 296 K): $\delta = 165.7$ (CN₃), 141.7, 136.7, 126.3, 125.7, 122.4, 113.8 (C_{Arom}), 40.9 (CH₃) ppm. MS (EI): m/z (%) = 532 (50) [M]⁺, 496 (20) [(tmgn)PdCl]⁺, 460 (77) [(tmgn)Pd]⁺. UV/Vis: $\lambda = 290, 355 \text{ nm}$. IR: $\tilde{\nu} = 1561$ [ν (C=N)] cm⁻¹. Crystal data for **1**: C₂₀H₃₀Cl₂N₆Pd·CH₂Cl₂, $M_r = 616.73$, $0.30 \times 0.10 \times 0.10 \text{ mm}$, monoclinic, space group $P2_1/c$, $a = 10.2408(8)$, $b = 16.5023(13)$, $c = 14.9271(12) \text{ \AA}$, $\beta = 95.456(2)^\circ$, $V = 2511.2(3) \text{ \AA}^3$, $Z = 4$, $d_{\text{calcd.}} = 1.631 \text{ Mg m}^{-3}$, $T = 100 \text{ K}$, θ range 1.8 to 26.4°. Reflections measured 46844, independent 5135 ($R_{\text{int}} = 0.0974$), observed [$I > 2\sigma(I)$] 3231, semiempirical absorption correction. Final R indices [$F_o > 4\sigma(F_o)$]: $R(F) = 0.0437$, $wR(F^2) = 0.0901$.

[(PS3)PtCl₂(C₂H₄)] (2**):** [PtCl(C₂H₄)(μ -Cl)]₂ (60 mg, 0.102 mmol) was dissolved in CH₂Cl₂ (10 mL). A solution of PS3 (71 mg, 0.2 mmol) in CH₂Cl₂ (10 mL) was then added dropwise over a period of 30 min. The yellow solution was stirred for additional 30 min at room temperature and the solvent was removed in vacuo afterwards. The remaining yellow powder was redissolved in toluene and filtered through silica. A yellow powder (83 mg) was obtained, which was washed several times with PE 40/60. Yellow crystals of **2** were grown at -20°C by layering a toluene solution with PE 40/60. ¹H NMR (399.89 MHz, CD₂Cl₂, 296 K): $\delta = 8.59$ (d, ¹J_{H-H} = 7.3 Hz, 1 H), 7.51–7.15 (m, 4 H), 6.16 (d, ¹J_{H-H} = 7.2 Hz, 1 H), 4.45 (m, ¹J_{Pt-H} = 82 Hz, 4 H), 3.76 (s, 3 H, CH₃), 2.90 (s, 15 H, CH₃), 2.63 (s, 3 H, CH₃), 1.96 (s, 3 H, CH₃) ppm. ¹³C NMR (100.56 MHz, CD₂Cl₂, 296 K): $\delta = 168.8$, 160.5 (CN₃), 150.1, 147.5, 137.0, 126.4, 125.6, 124.9, 124.8, 124.2, 121.0, 117.8 (C_{Arom}), 70.6 (C₂H₄), 41.1, 40.4 (br.), 39.6, 38.9 (CH₃) ppm. ¹⁹⁵Pt NMR (85.96 MHz, CD₂Cl₂, 296 K): $\delta = -2787$ (br.) ppm. MS (FAB): m/z (%): 649 (66) [M + H]⁺, 548 (100) [(tmgn)Pt]⁺, 620 (90) [(tmgn)-

PtCl_2^+ , 584 (68) [(tmgn)PtCl] $^+$. Crystal data for **2**: $\text{C}_{22}\text{H}_{34}\text{Cl}_2\text{N}_6\text{Pt}$, $M_r = 648.54$, $0.30 \times 0.10 \times 0.10$ mm, monoclinic, space group $P2_1/n$, $a = 10.619(2)$, $b = 15.451(3)$, $c = 15.965(3)$ Å, $\beta = 107.16(3)^\circ$, $V = 2502.8(9)$ Å 3 , $Z = 4$, $d_{\text{calcd.}} = 1.721$ Mg m $^{-3}$, Mo- K_α radiation (graphite monochromated, $\lambda = 0.71073$ Å), $T = 200$ K, $\theta_{\text{range}} 1.88$ to 27.50° . Reflections measured 11425, independent 5740, $R_{\text{int}} = 0.0603$, semiempirical absorption correction. Final R indices [$I > 2\sigma(I)$]: $R1 = 0.0391$, $wR2 = 0.0860$.

[(PS3)PtCl $_2$] (3): As for the preparation of **2**, [PtCl(C $_2$ H $_4$)(μ -Cl)] $_2$ (50 mg, 0.085 mmol) was dissolved in CH $_2$ Cl $_2$ (10 mL) and a solution of PS3 (86 mg, 0.243 mmol, 1.4 equiv.) in CH $_2$ Cl $_2$ (10 mL) was added dropwise over a period of 30 min. In contrast to the preparation of **2**, the reaction mixture was stirred for a period of 20 h under reflux. After removal of the solvent, the orange residue was redissolved in toluene and filtered through a silica frit. Complex **3** remained on the frit and was washed several times with toluene. It was then redissolved in CH $_2$ Cl $_2$ and removed from the silica. An orange powder was obtained after solvent removal. Orange crystals (25 mg, 24%) were grown at room temperature from a CH $_2$ Cl $_2$ solution layered with PE 40/60. $\text{C}_{20}\text{H}_{30}\text{Cl}_2\text{N}_6\text{Pt}$ (620.49): calcd. C 38.71, H 4.87, N 13.54; found C 38.65, H 4.89, N 12.89. ^1H NMR (399.89 MHz, CD $_2$ Cl $_2$, 296 K): $\delta = 7.44$ (d, $^1\text{J}_{\text{H-H}} = 8.1$ Hz, 2 H), 7.25 (t, $^1\text{J}_{\text{H-H}} = 7.8$ Hz, 2 H), 6.54 (s, $^1\text{J}_{\text{H-H}} = 7.5$ Hz, 2 H), 2.83 (s, 24 H, CH $_3$) ppm. ^{13}C NMR (100.56 MHz, CD $_2$ Cl $_2$, 296 K): $\delta = 165.8$ (CN $_3$), 142.5, 125.8, 122.0, 112.8 (C $_{\text{Arom.}}$), 40.814 (CH $_3$) ppm. ^{195}Pt NMR (85.96 MHz, CD $_2$ Cl $_2$, 296 K): $\delta = -1807$ (br.) ppm. MS (EI): m/z (%) = 620 (100) [M] $^+$, 548 (70) [(tmgn)PtCl] $^+$, 584 (32) [(tmgn)PtCl] $^+$. UV/Vis: $\lambda = 358$ (br.) nm. Crystal data for **3**: $\text{C}_{20}\text{H}_{30}\text{Cl}_2\text{N}_6\text{Pt} \cdot \text{CH}_2\text{Cl}_2$, $M_r = 705.420$, $0.40 \times 0.30 \times 0.30$ mm, monoclinic, space group $P2_1/c$, $a = 10.283(2)$, $b = 16.653(3)$, $c = 15.044(3)$ Å, $\beta = 96.46(3)^\circ$, $V = 2559.80$ Å 3 , $Z = 4$, $d_{\text{calcd.}} = 1.830$ Mg m $^{-3}$, Mo- K_α radiation (graphite monochromated, $\lambda = 0.71073$ Å), $T = 200$ K, $\theta_{\text{range}} 1.83$ to 27.73° . Reflections measured 11615, independent 5912, $R_{\text{int}} = 0.0643$, semiempirical absorption correction. Final R indices [$I > 2\sigma(I)$]: $R1 = 0.031$, $wR2 = 0.0847$.

[(btmgbp)PtCl $_2$ (C $_2$ H $_4$)] (5): [Pt $_2$ Cl $_4$ (C $_2$ H $_4$) $_2$] (100 mg, 0.17 mmol) dissolved in CH $_2$ Cl $_2$ (5 mL) was added dropwise to a solution of btmgbp (110.3 mg, 0.34 mmol) in CH $_2$ Cl $_2$ (1 mL). The reaction mixture was stirred for 1 h at room temperature. After removal of the solvent in vacuo, a yellow powder was obtained, which was washed three times with PE 40/60 (10 mL). Yield: 108.4 mg (47%). Needle-shaped crystals were grown by slow diffusion of PE 40/60 into a toluene solution of **5**. $\text{C}_{24}\text{H}_{36}\text{Cl}_2\text{N}_6\text{Pt}$ (674.58): calcd. C 42.73, H 5.38, N 12.46; found C 42.20, H 5.29, N 11.90. ^1H NMR (399.89 MHz, CD $_2$ Cl $_2$, 296 K): $\delta = 8.38$ (dd, $^3\text{J} = 8.0$, $^4\text{J} = 1.1$ Hz, 1 H, H11), 7.61 (dd, $^3\text{J} = 7.6$, $^4\text{J} = 1.46$ Hz, 1 H, H5), 7.3–7.2 (m, 1 H, H10), 7.20–7.13 (m, 1 H, H8), 7.10–7.02 (m, 1 H, H3), 6.99 (dt, $^3\text{J} = 7.60$, $^4\text{J} = 1.3$ Hz, 1 H, H9), 6.80 (dt, $^3\text{J} = 7.4$, $^4\text{J} = 1.2$ Hz, 1 H, H4), 6.47 (dd, $^3\text{J} = 8.0$, $^4\text{J} = 1.0$ Hz, 1 H, H2), 4.60–4.57 (m, $^2\text{J}_{\text{Pt-H}} = 53.0$ Hz, 2 H, H $_{\text{ethylene}}$), 4.39–4.36 (m, $^2\text{J}_{\text{Pt-H}} = 51.71$ Hz, 2 H, H $_{\text{ethylene}}$), 3.60 (s, 3 H, CH $_3$), 2.67 (s, 12 H), 2.59 (s, 3 H, CH $_3$), 2.41 (s, 3 H, CH $_3$), 2.21 (s, 3 H, CH $_3$) ppm. ^{13}C NMR (100.56 MHz, CD $_2$ Cl $_2$, 296 K): $\delta = 165.7$ (C13), 159.0 (C18), 149.7 (C1), 148.1 (C12), 134.8 (C7), 132.3 (C8), 131.0 (C5), 129.9 (C6), 129.4 (C11), 127.5 (C3), 126.8 (C10), 122.0 (C $_{\text{Aryl}}$), 121.9 (C $_{\text{Aryl}}$), 119.7 (C4), 71.6 (2 C, C $_2$ H $_4$), 41.5 (CH $_3$), 41.5 (CH $_3$), 40.1 (4 C, CH $_3$), 39.9 (CH $_3$), 39.4 (CH $_3$) ppm. ^{195}Pt NMR (85.96 MHz, CD $_2$ Cl $_2$, 296 K): $\delta = -2831$ ppm. MS (ESI $^+$): m/z (%) = 674.2 (100) [MH] $^+$, 673.2 (75) [M] $^+$. UV/Vis (CH $_2$ Cl $_2$): $\lambda = 281$ nm. Crystal data for **5**: $\text{C}_{24}\text{H}_{36}\text{Cl}_2\text{N}_6\text{Pt}$, $M_r = 674.58$, $0.35 \times 0.25 \times 0.20$ mm, monoclinic, space group $P2_1/c$, $a = 9.2180(18)$, $b = 19.928(4)$, $c = 15.569$ Å, $\beta = 105.10(3)^\circ$, $V = 2761.2(9)$ Å 3 , $Z = 4$, $d_{\text{calcd.}} = 1.623$ Mg m $^{-3}$, Mo- K_α radiation (graphite monochromated, $\lambda =$

0.71073 Å), $T = 200$ K, $\theta_{\text{range}} 1.70$ to 27.57° . Reflections measured 47990, independent 6340, $R_{\text{int}} = 0.0686$, semiempirical absorption correction. Final R indices [$I > 2\sigma(I)$]: $R1 = 0.0321$, $wR2 = 0.0734$.

Heck Reaction: NaOAc (360 mg, 4.4 mmol), styrol (0.64 mL, 5.6 mmol) and iodobenzene (0.445 mL, 4 mmol) were dissolved in dmf (5 mL). Subsequently, Pd complex **1** (8.5×10^{-3} mmol) was added. The reaction mixture was stirred for 5 h at ca. 135 °C. Subsequently, the reaction was stopped by addition of H $_2$ O (ca. 10 mL). The product was then extracted by addition (2 times) of CH $_2$ Cl $_2$ (ca. 15 mL). The CH $_2$ Cl $_2$ solution was shaken five times with H $_2$ O, dried with MgSO $_4$ and filtered. After removal of the solvent, *trans*-stilbene was obtained with more than 95% yield.

Hydrosilylation: Et $_3$ SiH (0.48 mL, 3 mmol) and Me $_3$ SiCHCH $_2$ (0.87 mL, 6 mmol) were dissolved in *n*-hexane (30 mL). Subsequently, the potential catalyst (complex **2** or **3**, 6×10^{-3} mmol) was added. The reaction (at 30 °C) was followed by GC/MS measurements. For these measurements, 0.1 mL of the reaction mixture was filtered through a silica frit. The product [Me $_3$ SiC(H)-CH $_2$ (SiEt $_3$)] was redissolved and removed from the silica with *n*-hexane (1 mL), before being injected into the GC/MS machine.

Supporting Information (see footnote on the first page of this article): NMR spectroscopic data of [btmgnH] $^+$ [PtCl $_3$ (C $_2$ H $_4$)] $^-$, IR spectra recorded for complexes **1** and **3**, UV/Vis spectra recorded for complexes **1** and **3**, and isodensity surfaces of the HOMOs and LUMOs of **2** and **3**

Acknowledgments

We gratefully acknowledge the Deutsche Forschungsgemeinschaft for their continuous financial support.

- [1] R. W. Alder, P. S. Bowman, W. R. S. Steele, D. R. Winterman, *Chem. Commun.* **1968**, 723–724.
- [2] T. Yamasaki, N. Ozaki, Y. Saika, K. Ohta, K. Goboh, F. Nakamura, M. Hashimoto, S. Okeya, *Chem. Lett.* **2004**, 33, 928–929.
- [3] S. N. Gamage, R. H. Morris, S. J. Rettig, D. C. Thackray, I. S. Thorburn, B. R. James, *J. Chem. Soc., Chem. Commun.* **1987**, 894–895.
- [4] M. A. Zirnstein, H. A. Staab, *Angew. Chem.* **1987**, 99, 460–461; *Angew. Chem. Int. Ed. Engl.* **1987**, 26, 460–461.
- [5] V. Raab, J. Kipke, R. M. Gschwind, J. Sundermeyer, *Chem. Eur. J.* **2002**, 8, 1682–1693.
- [6] a) R. W. Alder, *J. Am. Chem. Soc.* **2005**, 127, 7924–7931; b) B. B. Schneider, J. F. Grabowski, R. W. Alder, B. M. Foxman, L. Yang, *Can. J. Chem.* **2006**, 84, 1242–1249.
- [7] H.-U. Wüstefeld, W. C. Kaska, F. Schüth, G. D. Stucky, X. Bu, B. Krebs, *Angew. Chem.* **2001**, 113, 3280–3282; *Angew. Chem. Int. Ed.* **2001**, 40, 3182–3184.
- [8] S. Pohl, M. Harmjan, J. Schneider, W. Saak, G. Henkel, *J. Chem. Soc., Dalton Trans.* **2000**, 3473–3479.
- [9] S. Herres-Pawlis, A. Neuba, O. Seewald, T. Seshadri, H. Egold, U. Flörke, G. Henkel, *Eur. J. Org. Chem.* **2005**, 4879–4890.
- [10] C. Würtele, E. Gaoutchenova, K. Harms, M. C. Holthausen, J. Sundermeyer, S. Schindler, *Angew. Chem.* **2006**, 118, 3951–3954; *Angew. Chem. Int. Ed.* **2006**, 45, 3867–3869.
- [11] The best plane is obtained by minimizing the sum of the square deviations of all C atoms in the naphthyl group. The maximum deviations from this plane are 13.4(5) pm (C1) and –12.2(5) pm (C3) for **1**, and 14.7 pm (C1) and –12.3 pm (C3) for **3**. The root-mean-square deviations of fitted atoms are 9.98 pm for **1** and 10.74 pm for **3**.
- [12] DNMR Lineshape Analysis module as part of the Topspin software package, TOPSPIN 2.1, **2008**, Bruker Biospin.

- [13] F. R. Hartley, *Chem. Rev.* **1969**, *69*, 799–844.
- [14] R. A. Love, T. F. Koetzle, G. J. B. Williams, L. C. Andrews, *Inorg. Chem.* **1975**, *14*, 2653–2657.
- [15] L. S. Bartell, E. A. Roth, C. D. Hollowell, K. Kuchitsu, J. E. Young Jr, *J. Chem. Phys.* **1965**, *42*, 2683–2686.
- [16] U. Wild, P. Roquette, E. Kaifer, J. Mautz, O. Hübner, H. Wade-pohl, H.-J. Himmel, *Eur. J. Inorg. Chem.* **2008**, 1248–1257.
- [17] A. Peters, U. Wild, O. Hübner, E. Kaifer, H.-J. Himmel, *Chem. Eur. J.*, DOI: 10.1002/chem.200800244.
- [18] Quantum chemical calculations within the framework of density functional theory were performed with the program package TURBOMOLE.^[24] For all calculations, the B3LYP functional was used,^[25] which is based on a three-parameter functional by Becke^[26] and incorporates the correlation functional by Lee, Yang, and Parr.^[27] The structures of the different systems are optimized and vibrational frequencies are calculated analytically.^[28] The determination of the electronic energies used the def2-TZVP basis set.^[29] Zero point vibrational energies and thermodynamic contributions were obtained with the smaller def2-SV(P) basis set^[29] only.
- [19] See, for example: E. Peris, J. A. Loch, J. Mata, R. H. Crabtree, *Chem. Commun.* **2001**, 201–202.
- [20] P. Steffanut, J. A. Osborn, A. DeCian, J. Fisher, *Chem. Eur. J.* **1998**, *4*, 2008–2017.
- [21] a) G. M. Sheldrick, *SADABS*, Bruker AXS, **2004–2008**; b) DENZO–SMN, Data processing software, Nonius **1998**; <http://www.nonius.com>.
- [22] a) P. T. Beurskens, in: G. M. Sheldrick, C. Krüger, R. Goddard (Eds.), *Crystallographic Computing 3*, Clarendon Press, Oxford, UK, **1985**, p. 216; b) P. T. Beurskens, G. Beurskens, R. de Gelder, J. M. M. Smits, S. Garcia–Granda, R. O. Gould, *DIRDIF–2008*, Raboud University Nijmegen, The Netherlands, **2008**.
- [23] a) G. M. Sheldrick, *SHELXS–97*, University of Göttingen, **1997**; b) G. M. Sheldrick, *Acta Crystallogr., Sect. A* **2008**, *64*, 112.
- [24] a) R. Ahlrichs, M. Bär, M. Häser, H. Horn, C. Kölmel, *Chem. Phys. Lett.* **1989**, *162*, 165–169; b) O. Treutler, R. Ahlrichs, *J. Chem. Phys.* **1995**, *102*, 346–354.
- [25] P. J. Stephens, F. J. Devlin, C. F. Chabalowski, M. J. Frisch, *J. Phys. Chem.* **1994**, *98*, 11623–11627.
- [26] A. D. Becke, *J. Chem. Phys.* **1993**, *98*, 5648–5652.
- [27] C. Lee, W. Yang, R. G. Parr, *Phys. Rev. B* **1988**, *37*, 785–789.
- [28] P. Deglmann, F. Furche, R. Ahlrichs, *Chem. Phys. Lett.* **2002**, *362*, 511–518.
- [29] F. Weigend, R. Ahlrichs, *Phys. Chem. Chem. Phys.* **2005**, *7*, 3297–3305

Received: July 8, 2008
Published Online: August 26, 2008